



---

# IÉSEG WORKING PAPER

## 2008-ECO-17

---

### **Geometric Representation of the Mean-Variance-Skewness Portfolio Frontier Based upon the Shortage Function**

Kristiaan Kerstens\*, Amine Mounir\*\*, Ignace Van de Woestyne\*\*

\* CNRS-LEM (UMR 8179), IÉSEG School of Management

\*\*Hogeschool Universiteit Brussel, Brussels, Belgium

**November 2008**

**IÉSEG School of Management, Catholic University of Lille  
3, rue de la Digue, 59000 Lille, France**

**[www.ieseg.fr](http://www.ieseg.fr)**

**Tel: 33 (0)3 20 54 58 92**

**Fax: 33 (0)3 20 57 48 55**

# Geometric Representation of the Mean-Variance-Skewness Portfolio Frontier Based upon the Shortage Function\*

Kristiaan Kerstens<sup>†</sup>, Amine Mounir<sup>‡</sup>, Ignace Van de Woestyne<sup>§</sup>

November 17, 2008

## Abstract

The literature suggests that investors prefer portfolios based on mean, variance and skewness rather than portfolios based on mean-variance (MV) criteria solely. Furthermore, a small variety of methods have been proposed to determine mean-variance-skewness (MVS) optimal portfolios. Recently, the shortage function has been introduced as a measure of efficiency, allowing to characterize MVS optimal portfolios using non-parametric mathematical programming tools. While tracing the MV portfolio frontier has become trivial, the geometric representation of the MVS frontier is an open challenge. A hitherto unnoticed advantage of the shortage function is that it allows to geometrically represent the MVS portfolio frontier. The purpose of this contribution is to systematically develop geometric representations of the MVS portfolio frontier using the shortage function and related approaches.

KEYWORDS: shortage function, efficient frontier, mean-variance-skewness efficiency

**Warning: Please print the figures in color for evaluation purposes.**

## 1 Introduction

Mean-Variance (MV) portfolio theory (Markowitz (1952)) has been known to possess many theoretical difficulties. Indeed, as stated by numerous authors, this work is not consistent with the Von Neumann-Morgenstern axioms of expected utility theory unless either (i) asset prices follow normal probability distributions, or (ii) utility functions representing investor preferences are quadratic. However, starting from at least Mandelbrot (1963), empirical studies have repeatedly shown that asset returns and portfolio returns

---

\*We thank two referees, the editor and W. Briec for providing most constructive comments.

<sup>†</sup>IESEG School of Management, Lille, France, [k.kerstens@ieseg.fr](mailto:k.kerstens@ieseg.fr)

<sup>‡</sup>Hogeschool Universiteit Brussel, Brussels, Belgium, [amine.mounir@hubrussel.be](mailto:amine.mounir@hubrussel.be)

<sup>§</sup>Hogeschool Universiteit Brussel, Brussels, Belgium, [ignace.vandewoestyne@hubrussel.be](mailto:ignace.vandewoestyne@hubrussel.be)

distributions are widely non-normal (see Campbell, Lo and McKinlay (1997)). Furthermore, starting from Arditti (1975), Kraus and Litzenberger (1976), Kane (1982), among others, a multitude of studies has shown that investors reveal a preference for positive skewness by their willingness to pay a risk premium for positively skewed assets. Large scale studies using individual investor accounts indeed confirm that portfolio returns of underdiversified investors are substantially more positively skewed than those of diversified investors and that apparent mean-variance inefficiency of underdiversified investors is mainly explained by their willingness to sacrifice mean-variance efficiency for higher skewness exposure (see, e.g., Mitton and Vorkink (2007)). Traditional measures used to gauge portfolio performances (for instance, Sharpe (1966), Treynor (1965), and Jensen (1968) to name but the most well-known) are based on the Capital Asset Pricing Model (CAPM), which itself is a simplification of the MV model. Consequently, these measures all suffer from the aforementioned theoretical difficulties.

Despite these well-known limitations, financial theory, and especially portfolio theory as an important subject for applications, seems to remain somewhat reluctant to incorporate higher order moments in its development. While a variety of alternative criteria for higher order moments portfolio selection have been around in the literature (see Wang and Xia (2002)), there does not seem to emerge a universally accepted procedure so far. Following Briec et al. (2007), it is possible to distinguish between primal and dual methods to characterize Mean-Variance-Skewness (MVS) optimal portfolios.<sup>1</sup> For instance, Lai (1991) proposed a primal approach determining MVS portfolios via multi-objective programming that enjoyed quite some popularity in empirical studies (see, e.g., Chunnachinda et al. (1997), Prakash et al. (2003), and Sun and Yan (2003)). More recently, Yu et al. (2008) develop an alternative MVS method based upon neural networks which converge relatively more quickly compared with similar multi-objective optimization techniques. As just another example, Ryoo (2007) sets up a model minimizing semi-variance, while fixing a return target and a measure of skewness defined as a ratio of positive semi-variance to negative semi-variance. In face of the above difficulties, the quadratic approximation of expected utility being obsolete, many studies have attempted to approximate investor's utility by adding higher moments. One example is Jondeau and Rockinger (2006) who used a dual approach starting from a specification of the indirect MVS utility function determining optimal portfolios via its parameters reflecting preferences for return, risk and skewness. In addition to these attempts to break away from the MV model via some type of generic multi-moment approach, it is important to stress that a multitude of models is available that substitute another risk measure (e.g., semi-variance (or a variety of other lower partial moments), mean absolute deviation, quantile shortfall risk, Gini mean difference, etc.) into the traditional Markowitz bi-criteria model creating an entire family of mean-risk models.<sup>2</sup>

Based upon Briec et al. (2004) who were the first to connect the primal and dual approaches in the MV case, Briec et al. (2007) demonstrated that the shortage function can project any (in)efficient portfolio exactly on the three dimensional MVS portfolio frontier

---

<sup>1</sup>We limit ourselves here to the first three moments, though this taxonomy also applies to higher order moments.

<sup>2</sup>Quite a few of these proposals are motivated by the desire to linearize the portfolio optimization problem. In real-life financial decisions where portfolios must meet numerous additional constraints (minimum transaction lots, transaction costs, mutual funds characteristics, etc.) LP solvability is of obvious importance (see Mansini et al (2003) or Krzemienowski and Ogryczak (2005)).

and that this function is connected via duality to an indirect MVS utility function. In particular, starting from a given portfolio, this shortage function is an efficiency measure that looks for improvements in both mean and skewness and decreases in variance, concurring with general investor preferences. Thus, a given portfolio can either turn out to be efficient and part of the MVS frontier, or it may be inefficient and then the shortage function bridges the distance to the efficient frontier and provides an indication about its degree of inefficiency. This characteristic of the shortage function also makes it the perfect basis for visually representing portfolios and their frontier projections. However, the strengths and weaknesses of this new shortage function approach remain to be assessed in practice.

In a closely related, but less general approach, Joro and Na (2006) stressed the need for tools allowing for geometric representations of these MVS portfolio frontiers.<sup>3</sup> Indeed, an investor can only develop a clear idea about the position of certain MVS efficient portfolios and their relative desirability when he/she can see these efficient points in a three dimensional MVS space. Otherwise stated, investors can only formulate their preferences and the associated risk parameters if they can visualize the portfolio frontier set. It seems to have gone almost unnoticed so far that the shortage function has the added advantage of being capable to geometrically represent the MVS portfolio frontier.

To the best of our knowledge, this contribution is the first to systematically develop how the Briec et al. (2007) approach can be employed for visualization purposes. The idea of visualization is partially inspired by methods of reconstructing production frontiers (e.g., Hackman, Passy and Platzman (1994)). However, it is important to note that production possibility sets are convex polyhedra while portfolio frontier sets are not, which implies a fundamentally different approach. Our method consists of generating a sufficient number of points on the portfolio frontier to allow constructing a point cloud representation. Obviously, the quality of the resulting geometric representation depends on the number of reconstructed points, but also on the degree of homogeneity of the point distribution. Compared with the MV portfolio frontier, the representation of the MVS portfolio frontier is also computationally non-trivial since we transit from a curve in the two dimensional MV plane to a frontier surface in the three dimensional MVS space. Moreover, this transition implies moving from convex to non-convex optimization modeling. Jurczenko, Maillet and Merlin (2006) are the only contribution we are aware of that geometrically reconstructs MVS-Kurtosis portfolio frontiers using the shortage function, but these authors do not discuss any methodological issues underlying their geometric reconstruction. The main aim of this contribution is exactly to systematically explore the technical issues underlying the geometric reconstruction of MVS portfolio frontiers.

The remainder of the paper is organized as follows. Section 2 presents the models and the conceptual framework developed in Briec et al. (2007) as well as some extensions to visualize the MVS surface in three dimensions. Section 3 elaborates feasible strategies for the geometric representation of MVS portfolio sets. Furthermore, it illustrates some of the key differences between the MV and MVS frontiers, and in this sense it is complementary to results reported in Briec et al. (2007). Section 4 concludes the paper.

---

<sup>3</sup>Indeed, the general direction of improvement selected by Briec et al. (2007) can be interpreted as a generalization of the article by Joro and Na (2006) who only seek for improvements in variance.

## 2 Analyzing MVS Portfolios: Theoretical Framework and Basic Illustrations

In this section, we lay out the foundations for the programs used to compute the projections composing the MVS frontiers. Basically, we follow the non-parametric approach initiated for the MV case by Briec et al. (2004). This seminal contribution opened up new perspectives for portfolio performance measurement that have been extended in Briec et al. (2007) into MVS space. These authors have defined the shortage function as a measure of distance between the portfolios (or assets) under evaluation and the MVS Pareto frontier. This shortage function measures the maximum proportional reduction in risk, while return and skewness dimensions are increased in the same proportion to the initial assets. This section essentially summarizes the theoretical framework developed in Briec et al. (2007), except that we now allow for projections from observed and fictitious portfolios in MVS space.

### 2.1 Basic Definitions

We first develop some basic definitions. Assume the basic problem is to select a portfolio (or fund of funds) from  $n$  financial assets (or funds). A portfolio  $x = (x_1, \dots, x_n)$  is a vector of proportions in each of these  $n$  financial assets with  $\sum_{i=1}^n x_i = 1$ . Excluding short sales, one must impose the condition  $x_i \geq 0$  for all  $i \in \{1, \dots, n\}$ . In general, the set of admissible portfolios is written as follows:

$$\mathfrak{S} = \left\{ x \in \mathbb{R}^n; \sum_{i=1}^n x_i = 1, x \geq 0 \right\}. \quad (1)$$

Assets are characterized by an expected return  $E[R_i]$  for  $i \in \{1, \dots, n\}$ , by a covariance matrix  $\Omega$  with

$$\Omega_{ij} = \text{Cov}[R_i, R_j] = E[(R_i - E[R_i])(R_j - E[R_j])],$$

for  $i, j \in \{1, \dots, n\}$  and by a co-skewness tensor of rank three  $\Lambda$  with:

$$\Lambda_{ijk} = E[(R_i - E[R_i])(R_j - E[R_j])(R_k - E[R_k])],$$

for  $i, j, k \in \{1, \dots, n\}$ .

The return of portfolio  $x$  is defined by  $R(x) = \sum_{i=1}^n x_i R_i$ . The expected return of this portfolio  $x$ , its variance and its skewness are straightforwardly computed as follows:

$$E[R(x)] = \sum_{i=1}^n x_i E[R_i], \quad (2)$$

$$\text{Var}[R(x)] = E[(R(x) - E[R(x)])^2] = \sum_{i,j=1}^n x_i x_j \Omega_{ij}, \quad (3)$$

$$\text{Sk}[R(x)] = E[(R(x) - E[R(x)])^3] = \sum_{i,j,k=1}^n x_i x_j x_k \Lambda_{ijk}. \quad (4)$$

To condense notation, the function  $\Phi : \mathfrak{S} \longrightarrow \mathbb{R}^3$  defined by:

$$\Phi(x) = (E[R(x)], \text{Var}[R(x)], \text{Sk}[R(x)])$$

is introduced to represent the expected return, variance and skewness of a given portfolio  $x$ . In the remainder, an element of  $\mathbb{R}^3$  is called a MVS point. Thus, a MVS point can be the image by  $\Phi$  of a portfolio, or any arbitrary point in this three-dimensional space. It is useful to define the MVS *image* of  $\mathfrak{S}$  as the image  $\Phi(\mathfrak{S})$ , with

$$\Phi(\mathfrak{S}) = \{\Phi(x); x \in \mathfrak{S}\}.$$

This set can be extended by defining a MVS *disposal representation set* via:

$$\mathcal{DR} = \Phi(\mathfrak{S}) + (\mathbb{R}_- \times \mathbb{R}_+ \times \mathbb{R}_-). \quad (5)$$

For the purpose of gauging portfolio efficiency, we must define a subset of this representation set known as the *weakly efficient frontier*:

**Definition 2.1.** In the MVS space, the *weakly efficient frontier*, also called the *theoretical frontier*, is defined as:

$$\partial^W(\mathfrak{S}) = \{(M, V, S) \in \mathcal{DR}; (-M', V', -S') < (-M, V, -S) \Rightarrow (M', V', S') \notin \mathcal{DR}\}.$$

In brief, the weakly efficient frontier is the set of all MVS points that are not weakly dominated in this three dimensional space. This frontier is part of the boundary of the disposal representation set. This disposal representation set is itself an extension of the MVS image. Consequently, the theoretical frontier can contain points that are not attainable by an admissible portfolio (hence, the moniker “theoretical” frontier).

Of course, it is also possible to define a *strongly efficient frontier* as follows:

**Definition 2.2.** In the MVS space, the *strongly efficient frontier*, also shortened to *efficient frontier*, is defined as:

$$\begin{aligned} \partial^S(\mathfrak{S}) = \{ & (M, V, S) \in \mathcal{DR}; (-M', V', -S') \leq (-M, V, -S) \text{ and} \\ & (-M', V', -S') \neq (-M, V, -S) \Rightarrow (M', V', S') \notin \mathcal{DR}\}. \end{aligned}$$

The latter subset contains all MVS points that are not strictly dominated in this three dimensional space.

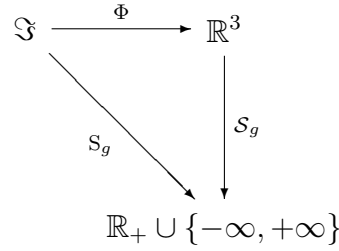
## 2.2 Shortage and Färe-Lovell Functions: Definitions, Basic Properties and Computational Issues

We now turn to an extended definition of the shortage function.

**Definition 2.3.** Let  $g = (g_M, g_V, g_S) \in \mathbb{R}_+ \times \mathbb{R}_- \times \mathbb{R}_+$  and  $g \neq 0$ . The shortage function  $\mathcal{S}_g$  in the direction of vector  $g$  is the function  $\mathcal{S}_g : \mathbb{R}^3 \rightarrow \mathbb{R}_+ \cup \{-\infty, +\infty\}$ , with

$$\mathcal{S}_g(y) = \sup_{\delta \in \mathbb{R}_+} \{\delta; y + \delta g \in \mathcal{DR}\}.$$

The relationship between this extended shortage function  $\mathcal{S}_g$  and the shortage function  $S_g$  introduced by Briec et al. (2004, 2007) is depicted in the following diagram:



Thus, for a given portfolio  $x \in \mathfrak{S}$ , it follows that  $S_g(x) = \mathcal{S}_g(\Phi(x))$ . Therefore,  $\mathcal{S}_g$  can indeed be seen as an extension since it allows to map arbitrary MVS points (including those not obtained from a portfolio). In the remainder, the extended shortage function is merely addressed as the shortage function.

The shortage function seeks simultaneously to improve return and skewness and to reduce the variance of a given MVS point in the direction of the vector  $g$ . Of key importance is that the shortage function respects sufficient conditions for a global optimum on non-convex MVS sets. Furthermore, the interpretation of the shortage function depends on the choice of direction vector. For instance, if the direction vector is chosen to be  $g = (|y_M|, -|y_V|, |y_S|)$  for the evaluated unit  $y = (y_M, y_V, y_S)$ , then this function has a proportional interpretation, which is convenient.

However, the use of this shortage function only guarantees that a projected MVS point is part of the weakly efficient subset. To ensure that the projection of a MVS point is part of the strongly efficient subset, one can make use of the recently introduced directional Färe-Lovell efficiency measure (see Briec (2000) for its general definition).<sup>4</sup>

**Definition 2.4.** Let  $g = (g_M, g_V, g_S) \in (\mathbb{R}_+ \setminus \{0\}) \times (\mathbb{R}_- \setminus \{0\}) \times (\mathbb{R}_+ \setminus \{0\})$ . The directional Färe-Lovell function  $\text{DFL}_g$  in the direction of vector  $g$  is the function  $\text{DFL}_g : \mathbb{R}^3 \rightarrow \mathbb{R}_+ \cup \{-\infty, +\infty\}$ , with

$$\text{DFL}_g(y) = \sup_{\beta \in \mathbb{R}_+^3} \left\{ \frac{1}{3} \sum_i \beta_i; y + \beta \odot g \in \mathcal{DR} \right\}.$$

Here,  $\odot$  denotes the Hadamard product of two vectors (i.e., the element by element product). This function is an extension of the Färe and Lovell (1978) efficiency measure. If the direction vector  $g = (|y_M|, -|y_V|, |y_S|)$  for the evaluated unit  $y = (y_M, y_V, y_S)$ , then this Färe-Lovell directional efficiency measure indicates the arithmetic average proportional change in all dimensions, making its interpretation slightly more complex in practice.

Given its key importance in this contribution, we clearly phrase the properties of the shortage and directional Färe-Lovell functions with respect to their projection onto the efficient frontiers.

**Proposition 2.1.** *The shortage function and the directional Färe-Lovell function project onto the weakly resp. the strongly efficient frontier:*

<sup>4</sup>He labels this the Russell proportional distance function.

1.  $\mathcal{S}_g(y) = 0 \Leftrightarrow y \in \partial^W(\mathfrak{S})$ ;
2.  $\text{DFL}_g(y) = 0 \Leftrightarrow y \in \partial^S(\mathfrak{S})$ .

*Proof.* For 1., see Bricc et al. (2007: Proposition 3.2 (a), page 139). For 2., analogous to Bricc (2000: page 196).  $\square$

It remains an open question to which extent the divergence between the weakly and the strongly efficient frontier, when using the shortage function, is empirically important when reconstructing portfolio frontiers. In the context of production frontiers, it is well-known that the shortage function leads to substantial amounts of deviations from the strongly efficient frontier (see, e.g., Ferrier, Kerstens and Vanden Eeckaut (1994) for an empirical illustration).

Following Bricc et al. (2007), the computation of the shortage function in MVS space in the direction of the vector  $g = (g_M, g_V, g_S)$  as specified in Definition 2.3 for a MVS point  $y = (y_M, y_V, y_S)$  under evaluation, can be obtained through solving the following cubic non-linear programming model:

$$\begin{aligned}
 & \max_{x, \delta} && \delta && \text{(P1)} \\
 & \text{s. t.} && \sum_{i=1}^n x_i = 1, \\
 & && \text{E}[R(x)] \geq y_M + \delta g_M, \\
 & && \text{Var}[R(x)] \leq y_V + \delta g_V, \\
 & && \text{Sk}[R(x)] \geq y_S + \delta g_S, \\
 & && \delta \geq 0, 0 \leq x_i \leq 1 \text{ for } i \in \{1, \dots, n\}.
 \end{aligned}$$

For clearness, we now introduce the notions of *efficient* and *theoretical projected points*:

**Definition 2.5.** For a given MVS point  $y = (y_M, y_V, y_S)$  under evaluation,

- the *efficient projected point* in the direction of vector  $g$  is the point in MVS space with coordinates determined by the left-hand sides of the inequality constraints of model (P1) evaluated at the optimal solution (i.e.,  $(\text{E}[R(x^*)], \text{Var}[R(x^*)], \text{Sk}[R(x^*)])$ );
- the *theoretical projected point* in the direction of vector  $g$  is the point in MVS space with coordinates determined by the right-hand sides of the inequality constraints of model (P1) evaluated at the optimal solution (i.e.,  $(y_M + \delta^* g_M, y_V + \delta^* g_V, y_S + \delta^* g_S)$ ).

We can easily see that the efficient projected point is merely the MVS point of the optimal portfolio obtained from model (P1).

If the shortage function equals zero, then the MVS point is part of the weakly efficient frontier. Otherwise, as can be seen from the right-hand sides of the inequality constraints of (P1), the optimal  $\delta$  indicates a change in return, variance and skewness that results in a projection of the evaluated MVS point onto the weakly efficient frontier.

The efficient projected point may differ from the theoretical projected point determined by the application of the shortage function to the MVS point under evaluation, because



of the existence of slack and surplus variables at the optimum. To be explicit, if slack and surplus variables occur at the optimum, this signifies that the shortage function resulting in the theoretical projected point underestimates the potential gains in return and skewness and the reduction in risk relative to the efficient projected point. Thus, the shortage function is potentially a downward biased efficiency measure in that it may underestimate the proportional gains in return and skew and the reduction in risk that are achievable at the efficient projected point. The upshot is that one should distinguish between a theoretical frontier, created by theoretical projected points, and the efficient frontier, that is feasible in practice and that is generated by efficient projected points. This divergence is due to the assumption of free disposal, which serves the sole purpose of facilitating the optimization process (see Bricc et al. (2004)).

In a similar way, to compute the Färe-Lovell function in MVS space into the direction of vector  $g = (g_M, g_V, g_S)$  as in Definition 2.4 for a MVS point  $y = (y_M, y_V, y_S)$  being evaluated, one can proceed as follows:

$$\begin{aligned}
 \max_{x, \beta} \quad & \frac{1}{3} \sum_{i=1}^3 \beta_i & (P2) \\
 \text{s. t.} \quad & \sum_{i=1}^n x_i = 1, \\
 & E[R(x)] \geq y_M + \beta_1 g_M, \\
 & \text{Var}[R(x)] \leq y_V + \beta_2 g_V, \\
 & \text{Sk}[R(x)] \geq y_S + \beta_3 g_S, \\
 & \beta_i \geq 0, 0 \leq x_i \leq 1 \text{ for } i \in \{1, \dots, n\}.
 \end{aligned}$$

If the Färe-Lovell function equals zero, then the MVS point is part of the strongly efficient frontier. If it is nonzero, then the optimal  $\beta_i$  indicate the proportional change per return, variance and skewness dimension that guarantees a projection of the evaluated MVS point onto the strongly efficient frontier.

Because of the higher flexibility of the Färe-Lovell function in choosing the projection direction, the slack and surplus variables are always zero at the optimum.<sup>5</sup> Consequently, the efficient and theoretical projected point of a MVS point under evaluation always

---

<sup>5</sup>In a portfolio context, let  $\delta$ ,  $\gamma_2$  and  $\gamma_3$  be real numbers such that  $\beta_1 = \delta$ ,  $\beta_2 = \delta\gamma_2$  and  $\beta_3 = \delta\gamma_3$  in model (P2). Then, this model can be rewritten as

$$\begin{aligned}
 \max_{x, \delta, \gamma_2, \gamma_3} \quad & \delta \frac{1}{3} (1 + \gamma_2 + \gamma_3) \\
 \text{s. t.} \quad & \sum_{i=1}^n x_i = 1, \\
 & E[R(x)] \geq y_M + \delta g_M, \\
 & \text{Var}[R(x)] \leq y_V + \delta\gamma_2 g_V, \\
 & \text{Sk}[R(x)] \geq y_S + \delta\gamma_3 g_S, \\
 & 0 \leq x_i \leq 1 \text{ for } i \in \{1, \dots, n\}.
 \end{aligned}$$

If  $\gamma_2$  and  $\gamma_3$  are fixed, then this model is equivalent to model (P1) but with the vector  $(g_M, \gamma_2 g_V, \gamma_3 g_S)$  as projection direction. However, since  $\gamma_2$  and  $\gamma_3$  are not fixed, the Färe-Lovell function clearly has more flexibility in choosing the projection direction in comparison to the shortage function.

coincide. It is well-known that the Färe-Lovell function is always larger than or equal to the shortage function (i.e.,  $\mathcal{S}_g(y) \leq \text{DFL}_g(y)$ : see, e.g., Färe and Lovell (1978)).

Notice that the shortage function approach encompasses three special cases that could also potentially be employed to reconstruct the MVS frontier: (i) a return maximization model, (ii) a risk minimization model, and (iii) a skewness maximization model. These models result from setting two coordinates of the direction vector  $g$  equal to zero (see Remark 3.4 in Briec et al. (2007: page 141)).

### 2.3 Illustration: Weakly and Strongly Efficient Subsets of the MVS Frontier

Figures 1a to 1d illustrate the proposed approach geometrically with artificial MVS points considered from four viewpoints. In each of these four figures, one three dimensional and three two dimensional, initial MVS points are represented by points ① and ④, while their efficient projected points using the shortage function are points ②, ③ and ⑤. The shortage function projects an arbitrary MVS point under evaluation onto the efficient frontier in the direction of an increased return, a reduced risk, and an increased skewness. This is illustrated in three dimensions in Figure 1a. This figure itself is projected orthogonally into its three natural two dimensional subspaces to clarify matters: Figures 1b, 1c, and 1d represent respectively the mean-variance, skewness-mean and skewness-variance dimensions.

The optimization process, situated in MVS space, is probably easiest to grasp on the latter three two dimensional figures. In Figure 1b, one observes that MVS points are projected to the upper left which indicates an improvement of return and a reduction of risk. In Figure 1c, one notices that initial MVS points are projected in the upper right direction resulting in an enhancement of both return and skewness. Finally, in Figure 1d, one observes that MVS points are again projected to the upper left, since skewness is improved upon while risk is being reduced.

Focusing now in more detail on a single MVS point, point ① is projected onto the efficient MVS point ③, while point ② is the theoretical projected point. Both points ② and ③ are generated by model (P1). The differences between these points ② and ③ reflect the possible slack and surplus variables at the optimum. Such difference between the efficient and the theoretical projected point can be avoided by employing the Färe-Lovell function rather than the shortage function.

### 2.4 MVS Utility Function and Efficiency Decomposition

Of course, there are a multitude of points on the weakly or strongly efficient subset. In case the investor can articulate his preferences with respect to the first three moments into a MVS utility function, then normally a single element from the strong efficient subset maximizes this direct MVS utility function (though multiple optimal solutions cannot be excluded). This direct MVS utility function for a given portfolio  $x \in \mathfrak{S}$  can be written as follows:

$$U(x; \mu, \rho, \kappa) = \mu E[R(x)] - \rho \text{Var}[R(x)] + \kappa \text{Sk}[R(x)], \quad (6)$$

where the parameters are positive (i.e.,  $(\mu, \rho, \kappa) > 0$ ).

Maximizing this direct mean-variance-skewness utility function  $U(x; \mu, \rho, \kappa)$  over all possible portfolios  $x \in \mathfrak{S}$  yields the indirect MVS utility function  $U^*(\mu, \rho, \kappa)$ :

$$\begin{aligned} \max_x \quad & \mu E[R(x)] - \rho \text{Var}[R(x)] + \kappa \text{Sk}[R(x)] & \text{(P3)} \\ \text{s. t.} \quad & \sum_{i=1}^n x_i = 1, \\ & 0 \leq x_i \leq 1 \text{ for } i \in \{1, \dots, n\}. \end{aligned}$$

Notice that traditionally  $\phi = \frac{\rho}{\mu} \geq 0$  represents the degree of absolute risk aversion and  $\psi = \frac{\kappa}{\rho} \geq 0$  is known as prudence.

The standard numerical methods used for maximizing this objective function do not guarantee to attain the global optimum, since this problem is non-convex. This difficulty leads Briec et al. (2007) to convexify the disposal representation set by imposing tangent iso-utility surfaces compatible with the set of admissible MVS portfolios. Furthermore, they define another shortage function computed on this convex representation set known as the hyper-shortage function. We denote this function here by  $\mathcal{S}_g$ . We refer the reader to Briec et al. (2007) for technical details.

However, it is important to stress that the shortage function to some extent dispenses the researcher from specifying detailed investor preferences. The traditional utility approach to select optimal portfolios becomes almost redundant, especially since one could wonder how investors could eventually formulate their preferences and the associated risk parameters if they cannot visualize the MVS frontier in the first place. Whence, the importance of proper visual reconstructions of the underlying MVS frontier.

Following Briec et al. (2007), it is useful to distinguish between the Overall, Allocative, Convexity and Portfolio Efficiency when evaluating the scope for improvements in portfolio management. We have the following definition:

**Definition 2.6.** With given investor preferences  $\mu$ ,  $\rho$  and  $\kappa$ , the overall efficiency (OE) index for a given portfolio  $x \in \mathfrak{S}$  is defined as the quantity:

$$\text{OE}_g(x; \mu, \rho, \kappa) = \frac{U^*(\mu, \rho, \kappa) - U(x; \mu, \rho, \kappa)}{\mu g_M - \rho g_V + \kappa g_S};$$

Allocative efficiency (AE) is the quantity:

$$\text{AE}_g(x; \mu, \rho, \kappa) = \text{OE}_g(x; \mu, \rho, \kappa) - \mathcal{S}_g(\Phi(x));$$

Convexity efficiency (CE) is the quantity:

$$\text{CE}_g(x) = \bar{\mathcal{S}}_g(\Phi(x)) - \mathcal{S}_g(\Phi(x));$$

Portfolio efficiency (PE) is given by the quantity:

$$\text{PE}_g(x) = \mathcal{S}_g(\Phi(x)).$$

Portfolio Efficiency only guarantees reaching a point on the non-convex primal portfolio frontier, not necessarily a point on the frontier maximizing the investor's indirect

MVS utility function. Convexity Efficiency measures the difference between the shortage functions computed on both the convex representation set and the initial non-convex representation set  $\mathcal{DR}$ . Allocative Efficiency measures the portfolio adjustment along the convexified portfolio frontier to achieve the maximum of the indirect MVS utility function. This may imply reshuffling an eventual Portfolio Efficient and Convexity Efficient portfolio in function of the parameters of the MVS utility function. Finally, Overall Efficiency ensures that all these ideals are achieved simultaneously. In particular,  $OE_g(x; \mu, \rho, \kappa)$  is the ratio of (i) the difference between optimal (indirect) and actual MVS utility, and (ii) the inner product of the direction vector  $g$  with the vector  $(\mu, -\rho, \kappa)$  normal to the MVS utility function.

Overall Efficiency is the strongest requirement, since it is simply defined as the sum of those component measures:

$$OE_g(x; \mu, \rho, \kappa) = AE_g(x; \mu, \rho, \kappa) + CE_g(x) + PE_g(x).$$

It ensures projections of assets that maximize the indirect MVS utility for given parameters of risk aversion and prudence, corresponding to an investor's preferences (see Bricet et al. (2007) for more details).

## 2.5 Illustration: Efficiency Decomposition

While so far, illustrations were based on arbitrary examples, from here onwards we aim at illustrating the key elements of MVS frontiers and the more traditional MV portfolio frontiers using a small sample of 29 assets being part of the Dow Jones index.<sup>6</sup>

Figure 2 illustrates in three dimensions the aforementioned efficiency taxonomy. Figure 2a shows a frontal view, while Figure 2b takes a perspective from the back. In Figure 2a the oblique plane on the left represents the investor's utility for arbitrarily fixed parameters of risk aversion and prudence, while the theoretical frontier stretches out to the bottom and to the right. Obviously, from the reverse perspective, Figure 2b is composed of the same utility plane to the right and the theoretical frontier moving out to the bottom and to the left.

For any given set of risk aversion and prudence parameters, one normally finds at least one tangency point between the indirect utility function and the MVS frontier (point ④). If an investor would hold a portfolio coinciding with point ④, then he would be perfectly efficient in all respects. However, a more typical case is an inefficient portfolio (for instance leading to point ①) that is situated in the interior of the MVS image. This inefficient point ① is projected onto the theoretical frontier at point ②. The distance between the points ① and ② represents the portfolio efficiency. Allocative efficiency measures the distance between the frontier point ② and its projection guaranteeing the maximum of the indirect MVS utility function at point ③. In this case, the overall efficiency is represented by the total distance between the point under evaluation ① and its projection on the utility surface ③. Thus, the overall efficiency is simply defined as the sum of the portfolio and the allocative efficiencies. Note that the issue of convexity efficiency is treated in detail below, while

---

<sup>6</sup>The computations are based on daily returns observed between 15 December 2000 and 1 October 2002.

the eventual convexity efficiency in Figure 2 is subsumed under the heading allocative efficiency.

Since it is plausible that investors can only formulate their preferences and the associated risk parameters if they can visualize the MVS frontier, the remainder of this contribution ignores the Overall and Allocative efficiencies and concentrates instead on the Portfolio efficiency in an effort to reconstruct the MVS frontier.

The Briec et al. (2007) article demonstrates that the shortage function applied to a MV model yields higher returns and lower risks than the same function applied to a MVS model, but the latter attempts to improve skewness while the former ignores the skewness altogether. Thus, while inefficiencies in the MV framework are higher than in the MVS model, this more powerful result of the MV model must be weighted against its complete negligence of the skewness dimension. In other words, the benefit of the MVS model is that it allows for a contraction of risk and improvement of return that is only slightly below the enhancements obtained by the use of the traditional MV model, while in the same time a substantial improvement in term of skewness can be realized. To develop some intuition, Table 1 illustrates the differences between the two aforementioned models at the individual and the sample level for these 29 assets of the Dow Jones index.

A remark on the choice of a direction vector when computing (P1) and (P2) is necessary. For a given unit  $y = (y_M, y_V, y_S)$  under evaluation, we opt for  $g = (|y_M|, -|y_V|, |y_S|)$  as direction vector. In so doing, we turn the shortage function into a proportional shortage function: return and skewness are proportionally increased, while variance is proportionally reduced. Since negative values, in particular for return and skewness, cannot be precluded, it is in fact necessary to use absolute values. The same choice is made for the Färe-Lovell function.

Table 1 reports some statistics for the return, variance and skewness of the 29 assets and their projections onto the efficient MV and MVS frontiers (columns 2 to 10). The projections with the MVS model clearly yield a higher skewness on average than the projections computed with the MV model. By contrast, average return and variance are clearly lower in case of the MVS model compared with the MV model. Notice that for 12 observations the results for MV and MVS models are identical.

To summarize this relative performance between MV and MVS models, we propose a new percentage difference-based indicator SkG (*skewness gain*) that represents a measure of trade-off between the gain/loss in terms of skewness relative to the minimal gain/loss in terms of either return or risk:

$$\text{SkG} = \sqrt[3]{\% \Delta \text{Sk}[R(x)]} - \min \left( |\% \Delta R[x]|, \sqrt{|\% \Delta \text{Var}[R(x)]|} \right).$$

The percentage differences in this indicator are measured w.r.t. the corresponding values obtained by the MV model. We believe this dimensionless indicator offers a useful tool to gauge the benefit of using the MVS versus the MV models: when this difference is positive (negative), the gain in skewness compensates (is overruled by) the common loss in return and/or risk.<sup>7</sup> The empirical results in Table 1 (column 11) indicate that on average this gain in skewness is 78.50%.

---

<sup>7</sup>By taking the minimum over the unit return and risk dimensions, this definition is compatible with minimal assumption by expressing a common loss. Of course, alternative definitions based on other operations are conceivable.

Furthermore, Table 1 reports the value of the shortage function for both MV and MVS models (columns 12 and 13). To formally test for the difference between the densities of both these shortage function in MVS versus MV models, we employ a test-statistic developed by Li (1996) and refined by Fan and Ullah (1999) that is valid for both dependent and independent variables and that asymptotically follows a standard normal-distribution.<sup>8</sup> The null hypothesis is simply that both distributions are identical; the alternative hypothesis is that they are different. This test statistic amounts to 2.93: thus, the null hypothesis can be rejected at the 1% significance level at least (2.33 is the critical value). Thus, comparing the shortage function between MVS and MV models, we conclude that these efficiency measures follow a different distribution. In other words, the increase in skewness indeed seems to be significant. The latter conclusion can also be inferred from the difference ( $\Delta$ ) between the shortage function in MV and MVS models in Table 1 (column 14) that measures the net impact of adding the skewness dimension to the basic MV model (see Bricc et al. (2007)).

For a more detailed explanation, we propose to focus on the differences between these two models starting from the underperforming asset *American International Group* from the same data set (asset number 5 in Table 1). Table 1 reports the return, variance and skewness (columns 2 to 4) and its projections according to the MV and MVS models (columns 5 to 10). The percent change in return, variance and skewness is presented in Table 2. The MV model allows an important contraction in risk of 72.58% and an enhancement in return by 88.46% compared with the variance and return parameters of the initial asset. However, this MV projected portfolio has decreased the skewness by 114.49% compared with the initial situation. In fact, the original positive skewness of 1.5169 is replaced by a negative portfolio skewness of  $-0.2198$  as can be seen from Table 1. By contrast, the MVS model has improved both return and skewness by 70.77% respectively 46.39%, and furthermore it manages to decrease risk by 46.39%. Applied to the asset *American International Group* the percentage difference-based indicator (SkG) yields a value of 125.37%.

As yet another detailed example, we illustrate the use of the direction vector for the underperforming asset Boeing Corp (asset number 10 in Table 1) characterized by an initial negative return and skewness. In the MV model, starting from a return of  $-0.0100$  and a variance of 2.7803, the shortage function yields a value of 0.5778 which results in a theoretical projected point with a return of  $-0.0042$  ( $= -0.0100 + 0.5778 \times 0.0100$ ) and a variance of 1.1739 ( $= 2.7803 - 0.5778 \times 2.7803$ ). Notice that the return direction has switched sign in view of the initial negative sign of the return. A similar reasoning could be developed for explaining its projection into the MVS case.

## 3 Geometric Representations of MVS Frontiers

### 3.1 Technical Aspects of Geometric Representations

This section is the first attempt to represent MV and MVS optimization results within a common framework using geometric representations. This common three dimensional

---

<sup>8</sup>For small samples, a bootstrap approximation can be employed.

representation should allow investors to judge whether the optimization of skewness, combined with the traditional optimization of mean and variance, yields more desirable results than the MV model on its own.

### 3.1.1 Basic Setup

Briefly commenting on the technicalities of these three dimensional reconstructions, the non-linear models (P1), (P2) and (P3) needed to generate the Figures 1 to 4 below are solved by means of sequential quadratic programming routines identical to the subroutine NPSOL described in Gill et al. (1986). MVS points are projected using the shortage function or the Färe-Lovell function onto the MVS frontier. The resulting point cloud is then scaled to fit into a fixed size cube (which is visible in each of these images) and visualized using OpenGL rendering techniques. An advantage of OpenGL is that it is possible to add additional geometrical objects like spheres, planes and cubes. For instance, a plane can be used to slice the surface, as is done in Figure 4.

Turning to strategies to develop three dimensional reconstructions of the potentially highly non-convex MVS frontiers introduced in Section 2, we distinguish between the use of three dimensional versus two dimensional grids. An initial strategy is to focus visualization on developing a three dimensional grid of MVS points contained within the empirical range of the return, risk and skewness dimensions of the basic set of observed portfolios. Conditional on this choice of a three dimensional grid, since the difference between weakly and strongly efficient frontiers is potentially important and has – to the best of our knowledge – never been investigated in a portfolio context, we explore the relative performance of the shortage function versus the Färe-Lovell function in this respect.

Figure 3a illustrates the MVS frontier obtained by projecting by means of the shortage function a three dimensional grid of  $50 \times 50 \times 50$  MVS points into a favorable direction (i.e., the standard direction vector that improves both return and skewness and reduces variance) determined by the relative position of the individual points in the grid. This projection approach results in a point cloud consisting of 125,000 three dimensional points. The combination of region ① and ② represents the theoretical MVS frontier. The geometric representation of this theoretical frontier is possible by the computation of the right-hand side of the cubic program (P1). The theoretical frontier can be subdivided into region ①, which consists of the right-hand side values with nonzero slack, and region ②, which contains the right-hand side values with zero slack.

Consequently, region ① consists of extreme values that actually cannot be reached by a feasible combination of assets, because of the nonzero slack in the inequalities. While this area is instrumental in computing the shortage (or similar) functions, it is obviously of no interest to an investor. By contrast, region ② represents optimal solutions with all zero slacks, which means that these portfolios can actually be reached in reality. Put differently, region ② can be seen as the left-hand side values of the inequalities in model (P1) at the optimum, since left- and right-hand side values are equal for this region. Therefore, this region represents the efficient MVS frontier. The boundary of this MVS frontier corresponds to the region ③, where the zero slack state of region ② transgresses into the nonzero slack state of region ①.

Another way of obtaining the efficient MVS frontier is by using the Färe-Lovell function.

Practically, this means that model (P2) is solved rather than model (P1). Because the direction in which the projection is performed is more flexible, model (P2) always leads to zero slack solutions on the strongly efficient frontier. For this model, the theoretical frontier and the efficient MVS frontier always coincide. In Figure 3b the darker colored points represent the efficient MVS frontier based on the Färe-Lovell function. Obviously, this region corresponds to the strongly efficient frontier obtained using the shortage function in region ② of Figure 3a. For reasons of comparison, this same frontier is also represented in Figure 3b as the lighter colored region. Obviously, both techniques essentially lead to the same MVS frontier.

### **3.1.2 Shortage and Färe-Lovell Functions: Slacks, Li-test and Differences in Projection Points**

However, to verify in detail the differences between projections using the shortage versus the Färe-Lovell function, it is necessary to dig into the question of the prevalence of slacks and surplus variables when employing the shortage function. The difference between the efficient projected points and the theoretical projected points in the cubic program (P1) have so far never been empirically explored. Statistics on the shortage versus the Färe-Lovell function in Table 1 reveal that these measures of efficiency only coincide for the efficient observations (7 out of 29), but that these are different for all others. In particular, the number of observations that is experiencing slacks in the return, variance and skewness dimensions amounts to 18, 11 respectively 18 (not reported in Table 1). We also formally test for the difference between both densities of the shortage and the Färe-Lovell function used within the same MVS model. The Li (1996) and Fan and Ullah (1999) test statistic has the value 3.87. Again, the null hypothesis of identical distributions can be rejected at at least the 1% significance level (critical value is 2.33). Finally, we report the mean absolute deviation (MAD), minimal, maximal and the range between the differences of the projection points of shortage and Färe-Lovell functions in Table 3. Notice first that the total number of feasible projected MVS points amounts to 70,639. One observes large differences between both functions in terms of these dispersion criteria. MAD for the return, variance and skewness is respectively 0.0485, 1.9514 and 3.0771. The minimal difference, maximal difference, and the range between the differences of these projection points of both functions confirm the same dispersion.

To explore matters more systematically, Table 4 reports counts on the various possible combinations of slack and surplus variables in a single and in two dimensions in the optimal solution of the shortage function for the projections of the three dimensional grid of 125,000 points mentioned earlier. Notice that the actual number of points reported is smaller than the maximal number of 125,000 because some of these lead to infeasibilities. Indeed, in total 76.67% of all 71,484 feasible projections based on the three dimensional grid reveal some form of slack. Given the doubt on the global optimality of the resulting solution, we consider it little informative to report further details on the amount of slack and surplus variables.

Concluding, the prevalence of slack and surplus variables in portfolio analysis seems to be important enough to maintain that the shortage function has the disadvantage as an efficiency measure that it underestimates the potential gains in return and skew and the reduction in risk achievable at the efficient projected point. The Färe-Lovell function



yields an unbiased estimate of portfolio performance and leads to substantially different projection points compared to the shortage function, but as stated earlier it has a more complicated interpretation.

### **3.1.3 Shortage and Färe-Lovell Functions: Differences in Visualizations**

Furthermore, noticeable differences can be observed in the respective visualizations resulting from the shortage versus the Färe-Lovell functions. First, as can be seen in Figure 3b, the shortage function yields a more homogeneously distributed cloud of projection points compared to the Färe-Lovell function, which typically seems to generate more clustered results. This clustering appears around a series of individual points as observed throughout the surface. Examples are, for instance, found in region ①; on the surface curves found in region ②; or in more condensed regions like ③. This phenomenon can intuitively be explained by the fact that the optimization performed by the Färe-Lovell function is more flexible in determining the direction in which to optimally project.

This flexibility is apparently important in practice, as can be illustrated in Table 5. This table provides some statistics w.r.t. the angles of the actual projection directions in MVS space of the previously mentioned three dimensional grid consisting of 125,000 points (from which some are infeasible), but measured in the MV-, SM- and SV-subspaces. Clearly, the variation in the real projection direction is much higher for the Färe-Lovell compared to the shortage function. This shows that the Färe-Lovell function actually exploits its extra flexibility over the shortage function. Moreover, one notices that the Färe-Lovell function more often leads to projection directions parallel to one of the coordinate axes. Both of these phenomena may well explain the clustering observed in Figure 3b.

Second, being more flexible in the projection direction also seems to have the advantage that areas of the efficient MVS frontier that are “less accessible” for the shortage function have a higher chance of being detected. For example, this effect can be observed in region ① in Figure 3b. This characteristic is clearly in favor of the method based on the Färe-Lovell function.

Having explored the differences between the shortage and the Färe-Lovell function, we conclude that if visualization is the ultimate goal of the exercise the shortage function performs better, since it produces a more homogeneously distributed point cloud. We remark that all these effects regarding the Färe-Lovell versus the shortage function are equally observed on other data sets, both real and artificial.

### **3.1.4 Grid Choice: 2D versus 3D**

Turning to the issue of selecting a starting grid, a different strategy in the visualization process is to start from a series of two dimensional grids rather than a single three dimensional network of grid points as hitherto employed. The detailed geometric representations of the MVS frontier, as seen for instance in Figures 4 and 5, are generated from planar two dimensional regular grids of MVS points, each with their initial return, variance and skewness. All MVS points in this grid, located parallel to one of the coordinate planes (either the MV-, MS-, or VS-plane), are then projected orthogonal to these grids using

one of the three corresponding special cases of the shortage function (see above) with an appropriate chosen direction vector (i.e., only one component is non-zero) resulting in a point cloud in MVS space. In fact, for the figures in this article three two dimensional grids consisting of  $100 \times 100$  points, parallel to each of the three coordinate planes, were projected in a direction orthogonal to the respective grids (e.g., for the MV grid, we project with a shortage function that maximizes the skewness solely by having a direction vector with the mean and variance directions set equal to zero). Thus, 30,000 points (three times 10,000 points) have been projected orthogonal to the grid in the MV-, MS-, and VS-planes.

We remark that only the shortage function is used as a projection model for these two dimensional grids. This is not only because of its superiority for visualization, as already mentioned, but also because the Färe-Lovell function in the current definition cannot be used for initial projection directions parallel to one of the coordinate axes. As can easily be seen from model (P2), in such cases the objective function may well become unbounded, indicating an ill-conceived mathematical program.<sup>9</sup>

Moreover, the computational time required to obtain the visualizations is roughly speaking proportional to the number of points being generated. Since the two dimensional grid approach leads to less, but more homogeneously distributed points compared with the three dimensional grid approach, one can also expect a positive effect on the CPU-time. Table 6 gives an overview of the time required to produce the frontiers visible in Figures 3, 5 and 4, used in this article.<sup>10</sup> Obviously, these expectations are confirmed: two dimensional grids save considerable CPU-time.

### 3.1.5 Concluding Comments

Wrapping up the developments in this section, we have shown by means of the prevalence of slack and surplus variables in portfolio analysis that the shortage function has the disadvantage to underestimate existing inefficiencies. By contrast, the Färe-Lovell function yields an unbiased estimate of portfolio performance, but has a more complicated interpretation. Nevertheless, the shortage function has its merits because it tends to yield more homogeneous geometric representations, despite its lack of flexibility to adjust the direction vector compared to the Färe-Lovell function. The latter can reveal certain minor parts hidden for the shortage function, but otherwise leads to a clustered representation. These observations are reinforced by the fact that three dimensional grids do not seem to work as well as a series of complementary two dimensional grids combined with orthogonal projections using a shortage function with suitably selected direction vectors (whereas the Färe-Lovell function cannot be applied in this context). Overall, we think the shortage function remains a very attractive tool both to gauge the performance of portfolios (despite its bias) and to represent the choices open to investors. This simply illustrates that theoretically superior solutions like the Färe-Lovell function need not always contribute to a specific practical goal (i.e., geometric representations).

---

<sup>9</sup>Briec (2000) proposes a refined definition of this the Färe-Lovell function allowing for zero components in the direction vector. In the case of a single projection dimension, shortage and Färe-Lovell functions would then coincide.

<sup>10</sup>These tests were performed on a Dell D810 Notebook equipped with an Intel Pentium M 770 Centrino 2.13 GHz CPU and 1 GB of RAM memory.

## **3.2 MVS Frontiers: Further Explorations and Relation to MV Frontier**

### **3.2.1 Non-Convexities in the MVS Strongly Efficient Subset**

Since the shortage function allows to geometrically represent the MVS frontier, the illustration of other aspects of the efficiency decomposition developed in section 2 becomes trivial. Indeed, to circumvent the non-convexity of the efficient MVS frontier, Bricc et al. (2007) convexified the disposal representation set by imposing iso-utility surfaces compatible with the set of admissible MVS portfolios. However, the computation of the hyper-shortage function defined relative to this non-convex efficient frontier is currently impossible. Therefore, one must content oneself to include the convexity efficiency measure into the allocative efficiency component. However, thanks to the geometric representation of the MVS frontier, it becomes possible to empirically illustrate the occurrence of a convexity efficiency component.

Figure 4 demonstrates the potential non-convexity of the efficient MVS frontier. In this figure, region ① represents the theoretical frontier. All projections reaching the global optimum are situated in the region ②. The straight line ③ represents the tangent iso-utility surface connecting two global optima from the MVS frontier and the convexity efficiency is simply the measure of the distance between the portfolios laying on the non-convex part and their projections onto this tangent line. Parts (a) and (b) illustrate a section parallel to the mean-skewness plane respectively the MV plane. Both parts of this figure also show in the zoomed box a 2-dimensional projection of this same straight line in the mean-skewness plane respectively the MV plane. It illustrates the potential danger of utility-based approaches to portfolio selection to get stuck with non-feasible solutions for the optimal portfolio vector. The extent to which this phenomenon could manifest itself is an empirical matter that remains to be explored.

### **3.2.2 MVS versus MV Strongly Efficient Subset**

Figure 5a illustrates the efficient MVS frontier (region ②) contrasted with the efficient MV frontier (region ③). It is now trivial to observe that the MV frontier overlaid on top of the efficient MVS frontier forms a kind of lower bound along the skewness dimension. Indeed, all MVS points projected onto the efficient MVS frontier, are dominated by the efficient MV frontier in terms of the return and variance dimensions. However, the MVS model allows higher skewness for projections slightly different from the MV portfolios in terms of the same characteristics.

In the same figure, the theoretical frontier (i.e., region ①) is clearly visible. Compared with the visualization of this frontier in Figure 3a, we observe that visualization results improve if the reconstruction is based on two dimensional grids instead of three dimensional grids.

### **3.2.3 MVS Strongly Efficient Subset: Concentration and Diversification**

During the optimization process, additional data such as the proportions in the optimal portfolio and the values of the left-hand and right-hand sides of the constraints is com-

puted and stored. This data is then converted when needed to a proper form. For instance, the number of nonzero proportions in the optimal portfolio can be converted to a color hue between blue (low value) and red (high value) to obtain the result in Figure 5b.

Figure 5b represents the same efficient MVS frontier, but this time colored according to the number of (nonzero) assets actually contained in the optimal portfolios. We can mainly distinguish between three areas. Region ① is rather small and contains portfolios composed of the highest number of nonzero assets. This area simply illustrates the statistical fact that portfolios with a small variance must contain a large number of assets in an effort to diversify away risk. By contrast, region ③ constitutes by far the largest area and solely consists of portfolios containing “few” assets (3 to 4 at the most). Region ②, situated in between these regions (① and ③), is rather small and consists of all solutions in between in terms of the number of assets in the optimal solution. In fact, this figure illustrates that moving beyond the MV frontier almost inevitably implies a drastic change in investment strategy. Instead of seeking diversification over a wide set of assets (which only leads to the relatively small regions ① and ②), investors should try to carefully pick a rather small set of assets delivering superior performance in terms of skewness (the whole of region ③). Thus, to explore the whole of the MVS frontier one should unlearn the main lesson of Markowitz, namely diversification. The relative small area of diversified portfolios relative to the size of the MVS frontier could also contribute to explaining the widespread phenomenon of underdiversified portfolios (which in the literature has been linked to investor preferences for positive skewness (e.g., Kraus and Litzenberger (1976))).

### **3.2.4 MVS Strongly Efficient Subset: Cases with Shorting and Risk-Free Rate**

As an illustration of the generality of the proposed approach, we finally present examples of portfolio frontiers that are of practical value to the investment community, namely the case of shorting and the case when a risk-free asset is available.

Figure 6 represents the results of MV and MVS efficient frontiers without shorting with the same frontiers allowing to sell short. In part (a), the MVS frontier resulting from a shorting strategy is represented by region ②, while the MVS frontier without shorting generates region ①. Shorting allows for a more dispersed frontier, yielding gains in terms of return, variance and skewness in the projected portfolios. Thus, for a given level of variance, both return and skewness of a projected portfolio with shorting are higher than the ones of an MVS portfolio without shorting. Indeed, shorting consists of weighting negatively the rather non-desirable assets according to the MVS criteria, which allows leverage power to positively overweight the more desirable assets into the efficient portfolios. Figure 6b projects both MVS frontiers onto the MV plane. Here, shapes ① and ② represent the MV efficient frontiers with shorting respectively without shorting, whereby the former obviously dominates the latter.

Finally, Figure 7 contrasts efficient projected portfolios for MV and MVS models with and without a risk-free rate (RFR) of 2%. In part (a), the MVS frontier including the RFR is represented by the region ② and the same frontier without RFR constitutes the region ①. Notice that the MVS frontier with RFR extends MVS without RFR into the direction of the RFR (point ③). As in the MV case, including the RFR enlarges the set of efficient portfolio possibilities within certain ranges into the direction of a reduced variance

for given return and skewness, and into the direction of an increased skewness for given return and variance. Since the MV frontier is a lower bound to the MVS efficient frontier along the skewness dimension, the same interpretation remains valid when including the RFR. Indeed, Figure 7b shows a projection onto the MV plane, region ① and ② represent the MV frontier without respectively with RFR. The difference in both frontiers results solely from including the RFR, whereby the MV frontier with RFR offers for a given return level lower variance compared to the MV case without RFR.

### 3.2.5 Concluding Comments

Furthermore, the figures shown in this empirical illustration as well as numerous other runs we have made on both real and artificial data sets reveal that there does not seem to be such a thing as a typical shape for the efficient MVS frontier. Thus, it seems impossible for now to predict its shape purely on the basis of the initial statistical information contained in the data. We can however reconstruct the MVS frontier using computer-intensive optimization strategies using well-chosen grids.

Finally, we remark that special care must be taken because of the non-convex nature of these non-linear portfolio models. If a local optimum is not the global optimum, this often seems to lead to certain artifacts in the figures. In Figures 3a and 3b, for instance, this phenomenon can be observed near the upper part of the frontier at ④. In fact, there is a small part of the frontier missing since the optimization process fails to find the global optimum in that neighborhood. One strategy to reduce this phenomenon is to use different starting points for the numerical optimization process, but success in this venture is not guaranteed. From several empirical experiments both on real and artificially generated data sets, we conclude that in most cases the local optima obtained are in fact also global optima, especially in the regions of interest to an investor.

## 4 Conclusions

This paper has introduced a geometric representation of the MVS frontier related to a new tool introduced in the literature by Briec et al. (2007). This proposal could render great services to practitioners in portfolio management. This three dimensional representation of the efficient MVS frontier allows investors to just pick up a portfolio that matches suitably their needs in term of absolute risk aversion and absolute prudence. This contribution is based upon the shortage function introduced in the investment framework as a measure of performance. Our choice of this method as a tool for geometric representation is motivated by the fact that it approximates the true frontier via a non-parametric measurement through the risk contraction and the expansion of return and skewness. Furthermore, this shortage function has the advantage of presenting a general framework compatible with general investor preferences, while there is a plethora of alternative approaches (e.g., the multi-objective programming method of Lai (1991), the closely related MVS approach of Joro and Na (2006) focusing on variance reduction solely, ...) attempting to solve the MVS portfolio by privileging one or two parameters at the cost of the other dimension(s).

In the third section, different strategies to geometrically represent efficient MVS frontiers

are elaborated. In particular, both shortage and Färe-Lovell functions as well as the use of three- versus two-dimensional grids have been explored. The prevalence of slack and surplus variables in portfolio analysis reveals that the shortage function underestimates inefficiencies, while the Färe-Lovell function generates no such bias. On the other hand, when the direction vector is determined by the evaluated unit, the proportional interpretation of the shortage function is relatively easier than the arithmetic average interpretation of the Färe-Lovell function. In addition, the shortage function is meriting in developing geometric representations because of their homogeneity. The Färe-Lovell function leads to a clustered representation, though it can reveal parts of the MVS frontier that remain hidden for the shortage function. Furthermore, visualization using several two dimensional grids based on a shortage function with suitably selected direction vectors (the Färe-Lovell function is not applicable in this context) yields better results compared to a three dimensional grid. Moreover, this combination has the most favorable CPU-time. In conclusion, we think that the shortage function has advantages both when gauging the performance of portfolios (despite its bias) and when representing the MVS frontier from which investors may choose.

Furthermore, key differences between the MVS and MV frontiers have been illustrated. Portfolio efficiency in a MV framework is always greater than efficiency in the MVS framework, because one simply adds another (i.e., skewness) constraint. Geometrically, this result appears markedly, since the MV frontier represents a lower bound frontier on the efficient MVS frontier in terms of the skewness dimension. Furthermore, it is striking that large parts of the MVS frontier require only a small combination of assets rather than a diversification strategy.

We hope that the geometric representation of MVS portfolios may offer a tool to academics to explore a variety of additional questions related to portfolio choice (for instance, it may help to estimate the risk-aversion and prudence characterising investor preferences (e.g., Eisenhauer and Ventura (2003))). Equally so, this new development may well contribute to the dissemination of MVS optimization tools among practitioners (whom at least partly seem to be using large scale MV models (e.g., Perold (1984))). For instance, one may conjecture that the transaction and management costs of such portfolios are lower than in the traditional MV model. Of course, we do not pretend that this MVS model would provide an answer to all objections formulated by financial analysts to the standard MV model (for example, to maximize the estimation errors in the returns and variances, unstable optimal solutions, etc. (see, e.g., Michaud (1989))). These and many other questions remain to be tackled in future work.

## References

- [1] Arditti, F.D., Skewness and Investors' Decisions: A Reply, *Journal of Financial and Quantitative Analysis*, 10, (1975), 173–176.
- [2] Briec, W., K. Kerstens, J.-B. Lesourd, Single Period Markowitz Portfolio Selection, Performance Gauging and Duality: A Variation on the Luenberger Shortage Function, *Journal of Optimization Theory and Applications*, 120, (2004), 1–27.

- [3] Briec, W., K. Kerstens, O. Jokung, Mean-Variance-Skewness Portfolio Performance Gauging: A General Shortage Function and Dual Approach, *Management Science*, 53, (2007), 135–149.
- [4] Briec, W., An Extended Färe-Lovell Technical Efficiency Measure, *International Journal of Production Economics*, 65, (2000), 191–199.
- [5] Campbell, J. , A. Lo, A. McKinlay, The Econometrics of Financial Markets, *Princeton University Press, Princeton*, (1997).
- [6] Chunchinda, P., K. Dandapani, S. Hamid, A. J. Prakash, Portfolio Selection and Skewness: Evidence from International Stock Markets, *Journal of Banking and Finance*, 21, (1997), 143–167.
- [7] Eisenhauer, J.G., L. Ventura, Survey Measures of Risk Aversion and Prudence, *Applied Economics*, 35, (2003), 1477–1484.
- [8] Fan, Y., A. Ullah, On Goodness-of-fit Tests for Weakly Dependent Processes Using Kernel Method, *Journal of Nonparametric Statistics*, 11, (1999), 337–360.
- [9] Färe, R., C.A.K. Lovell, Measuring the Technical Efficiency of Production, *Journal of Economic Theory*, 19, (1978), 150–162.
- [10] Ferrier, G., K. Kerstens, P. Vanden Eeckaut, Radial and Nonradial Technical Efficiency Measures on a DEA Reference Technology: A Comparison using US Banking Data, *Recherches Économiques de Louvain*, 60, (1994), 449–479.
- [11] Gill, P.E., W. Murray, M.A. Saunders, M.H. Wright Users’ guide for NPSOL (Version 4.0): a Fortran package for nonlinear programming, Report SOL 86-2 Department of Operations Research, *Stanford University*, (1986).
- [12] Hackman, S., U. Passy, L. Platzman, Explicit Representation of the Two-Dimensional Section of a Production Possibility Set, *Journal of Productivity Analysis*, 5, (1994), 161–170.
- [13] Jensen, M., The Performance of Mutual Funds in the Period 1945-1964, *Journal of Finance*, 23, (1968), 389–416.
- [14] Jondeau, E., M. Rockinger, Optimal Portfolio Allocation under Higher Moments, *European Financial Management*, 12, (2006), 29–55.
- [15] Joro, T., P. Na, Portfolio Performance Evaluation in Mean-Variance-Skewness Framework, *European Journal of Operational Research*, 175, (2006), 516–542.
- [16] Jurczenko, E., B. Maillet, P. Merlin, Hedge Funds Portfolio Selection with Higher-order Moments: A Nonparametric Mean-Variance-Skewness-Kurtosis Efficient Frontier, in: *E. Jurczenko, B. Maillet (eds.) Multi-moment Asset Allocation and Pricing Models*, New York, Wiley, (2006), 51–66.
- [17] Kane, A., Skewness Preference and Portfolio Choice, *Journal of Financial and Quantitative Analysis*, 17, (1982), 15–25.
- [18] Kraus, A., R.H. Litzenberger, Skewness Preference and the Valuation of Risky Assets, *Journal of Finance*, 31, (1976), 1085–1100.

- [19] Krzemienowski, A. , W. Ogryczak, On Extending the LP Computable Risk Measures to Account Downside Risk, *Computational Optimization and Applications*, 32, (2005), 133–160.
- [20] Lai, T.Y., Portfolio Selection with Skewness: A Multiple-Objective Approach, *Review of Quantitative Finance and Accounting*, 1, (1991), 293–305.
- [21] Li, Q., Nonparametric Testing of Closeness between Two Unknown Distribution Functions, *Econometric Reviews*, 15, (1996), 261–274.
- [22] Mandelbrot, B., The Variation of Certain Speculative Prices, *Journal of Business*, 36, (1963), 394–419.
- [23] Mansini, R., W. Ogryczak, M.G. Speranza, LP Solvable Models for Portfolio Optimization: A Classification and Computational Comparison, *IMA Journal of Management Mathematics*, 14, (2003), 187–220.
- [24] Markowitz, H., Portfolio Selection, *Journal of Finance*, 7, (1952), 77–91.
- [25] Michaud, R.O., The Markowitz Optimization Enigma: Is 'Optimized' Optimal?, *Financial Analysts Journal*, 45, (1989), 31–42.
- [26] Mitton, T., K. Vorkink, Equilibrium Underdiversification and the Preference for Skewness, *Review of Financial Studies*, 20, (2007), 1255–1288.
- [27] Perold, A.F., Large-Scale Portfolio Optimization, *Management Science*, 30, (1984), 1143–1160.
- [28] Prakash, A.J., C.-H. Chang, T.E. Pactwa, Selecting a portfolio with skewness: Recent evidence from US, European, and Latin American equity markets, *Journal of Banking and Finance*, 27, (2003), 1375–1390.
- [29] Ryoo, H.S., A Compact Mean-Variance-Skewness Model for Large-Scale Portfolio Optimization and its Application to the NYSE Market, *Journal of the Operational Research Society*, 58, (2007), 505–515.
- [30] Sharpe, W., Mutual Fund Performance, *Journal of Business*, 39, (1966), 119–138.
- [31] Sun, Q., Y. Yan, Skewness Persistence with Optimal Portfolio Selection, *Journal of Banking and Finance*, 27, (2003), 1111–1121.
- [32] Treynor, J.L., How to Rate Management of Investment Funds, *Harvard Business Review*, 43, (1965), 63–75.
- [33] Wang, S.Y., Y.S. Xia, Portfolio Selection and Asset Pricing, *Lecture Notes in Economics and Mathematical Systems*, 514, (2002), Springer-Verlag.
- [34] Yu, L., S. Wang, K.K. Lai, Neural Network-Based Mean-Variance-Skewness Model for Portfolio Selection, *Computers & Operations Research*, 35, (2008), 34–46.



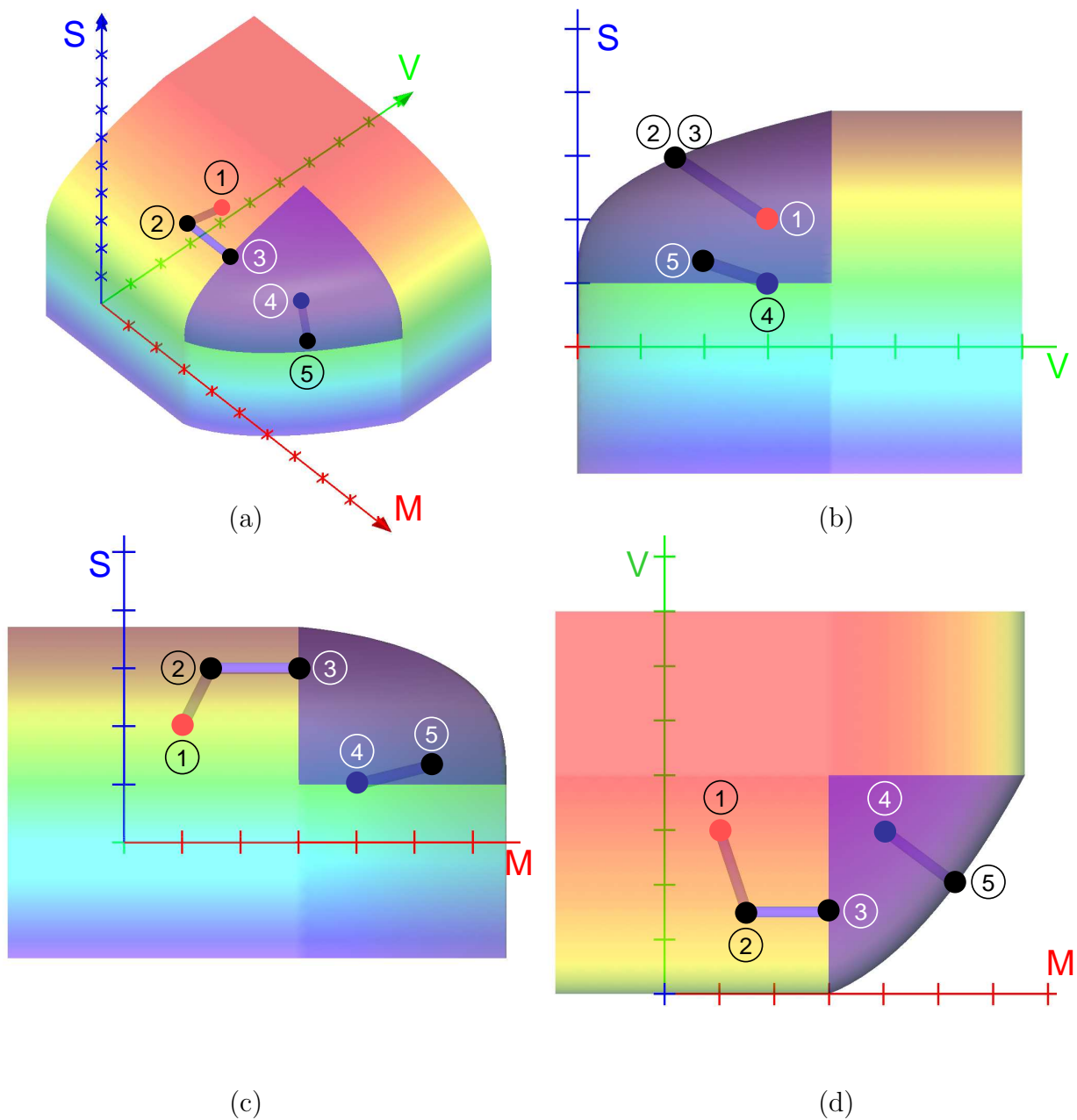


Figure 1: Projections onto the MVS frontier

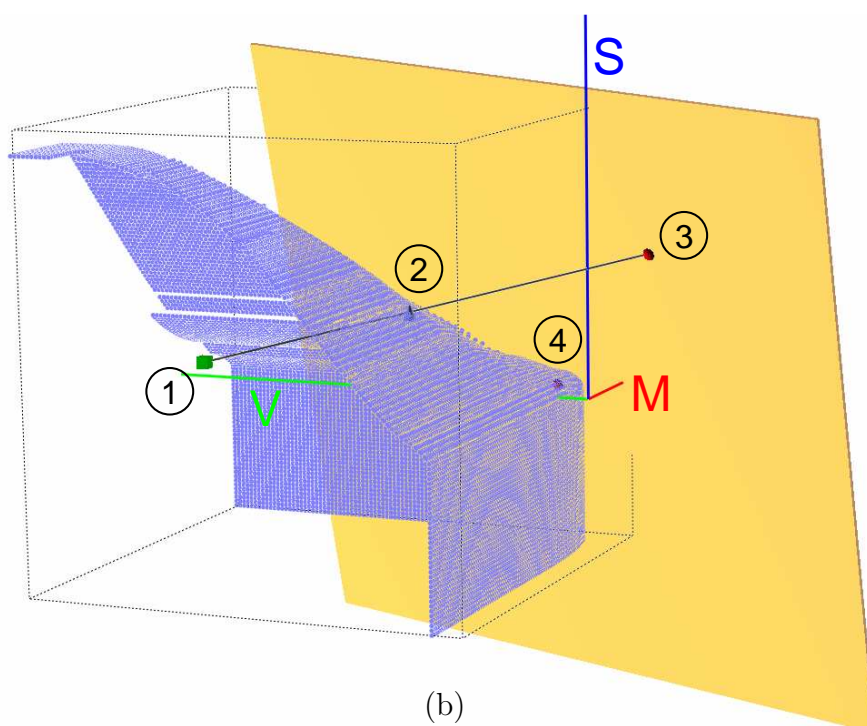
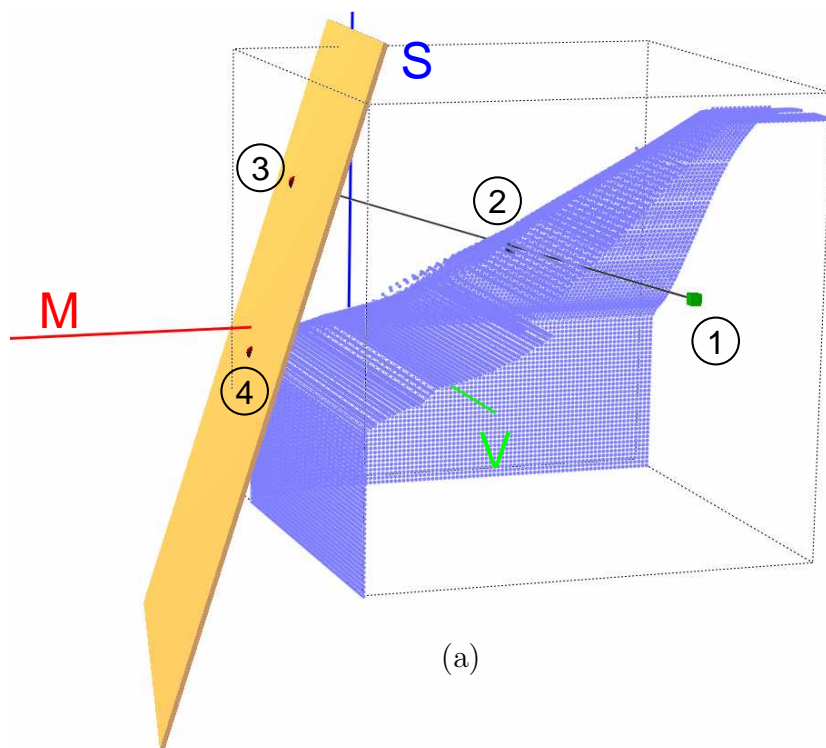
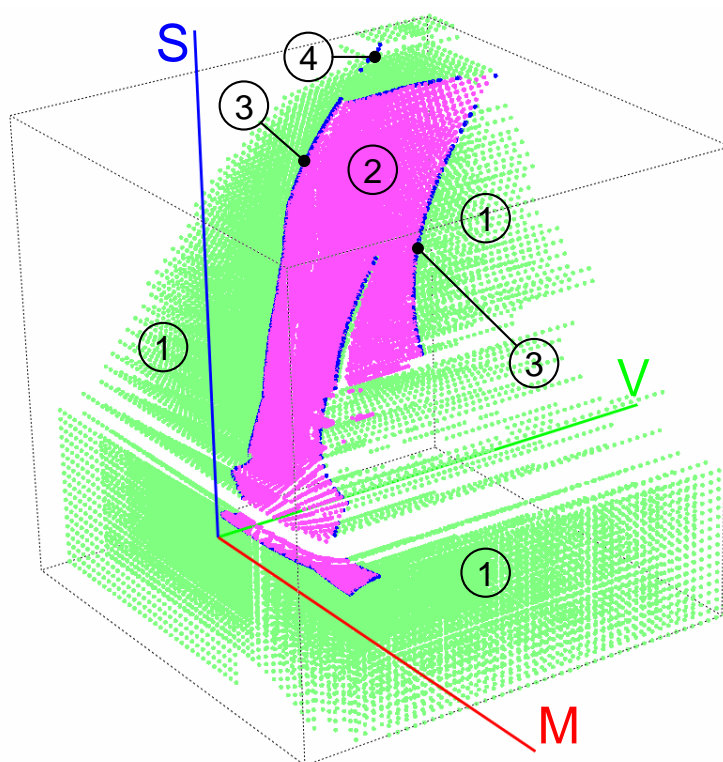
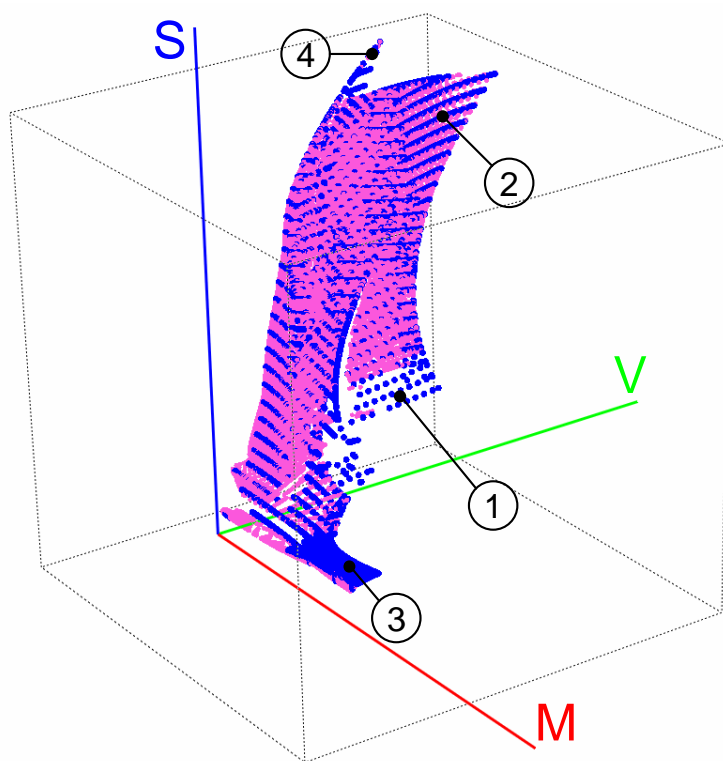


Figure 2: Theoretical MVS frontier with the MVS indirect utility function



(a)



(b)

Figure 3: The efficient frontier and the shortage function versus the Färe-Lovell function

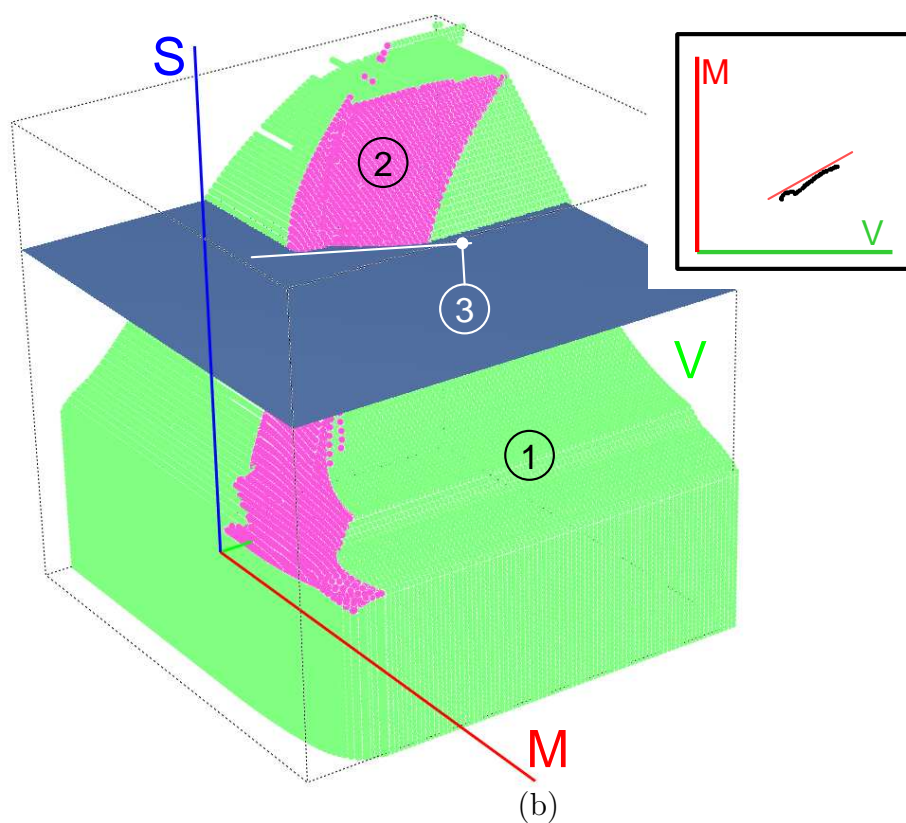
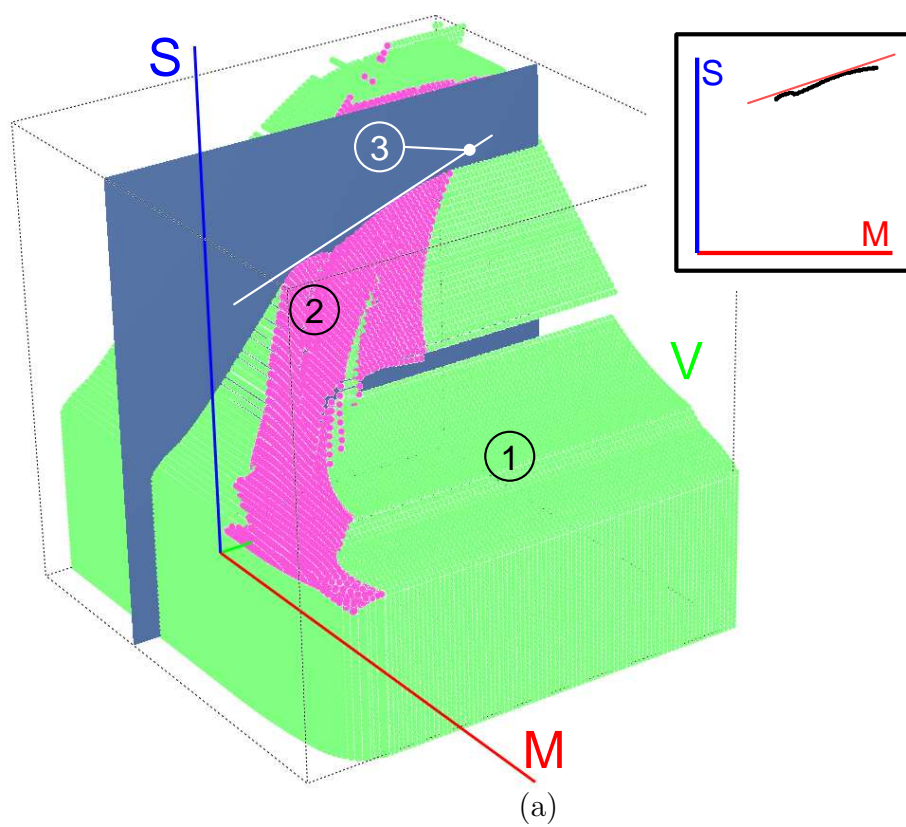
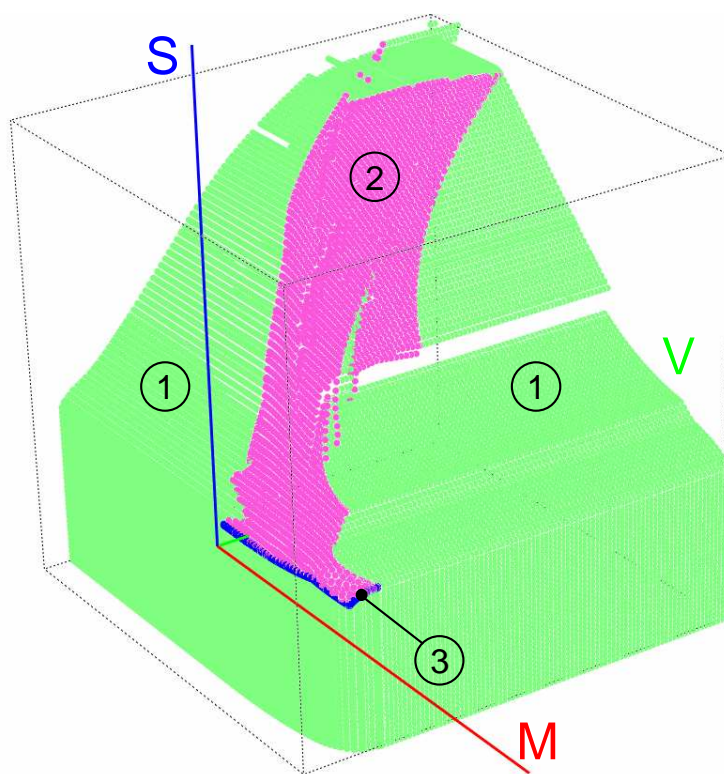
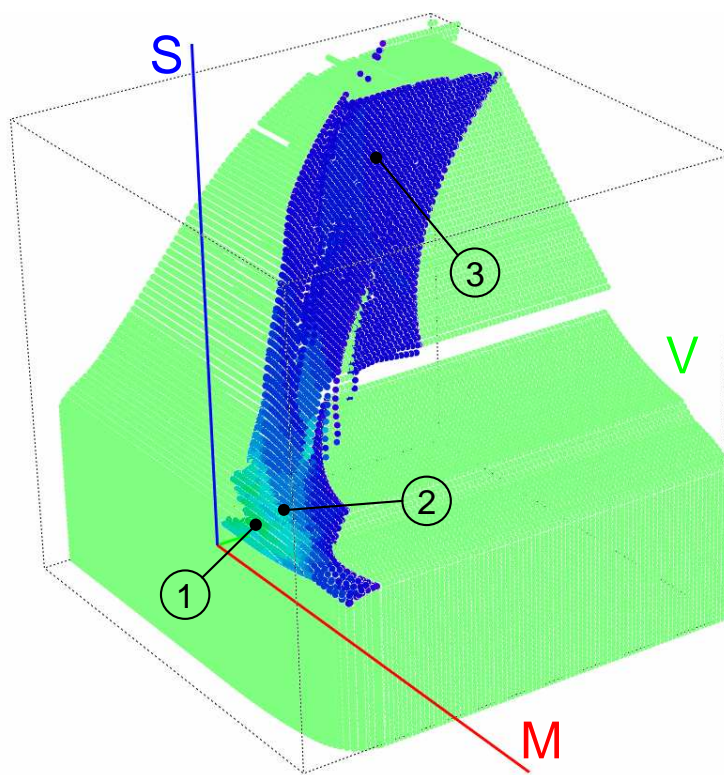


Figure 4: Convexity efficiency in the primal MVS frontier



(a)



(b)

Figure 5: MVS versus MV frontiers and effect of diversification

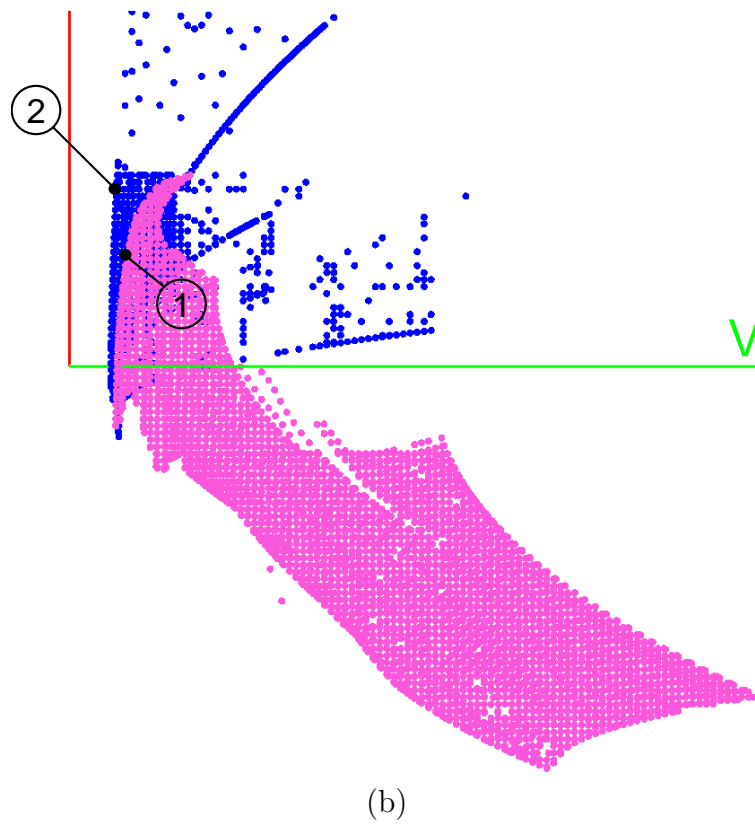
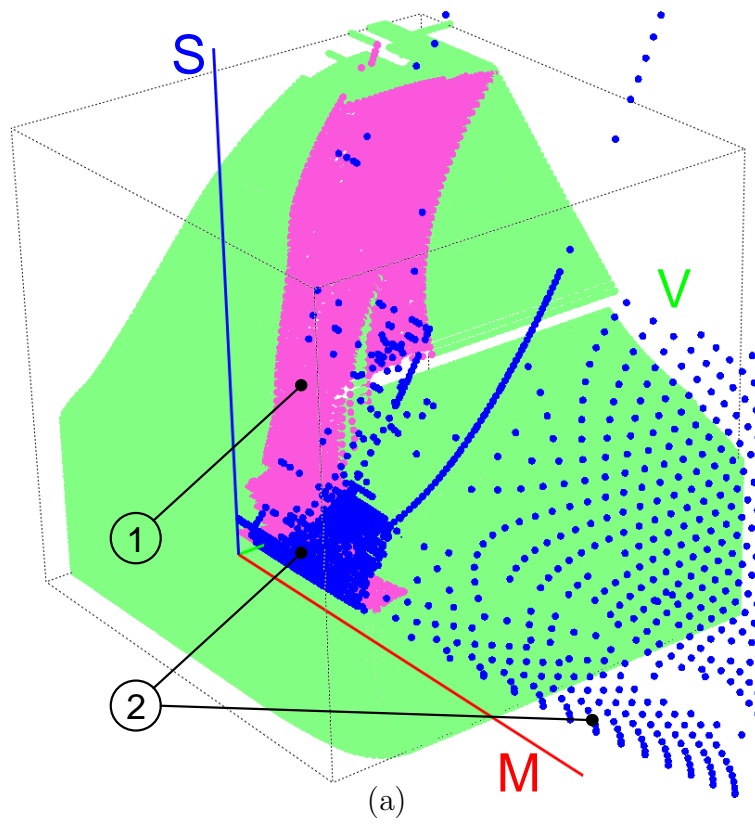


Figure 6: MV and MVS frontiers without and with shorting

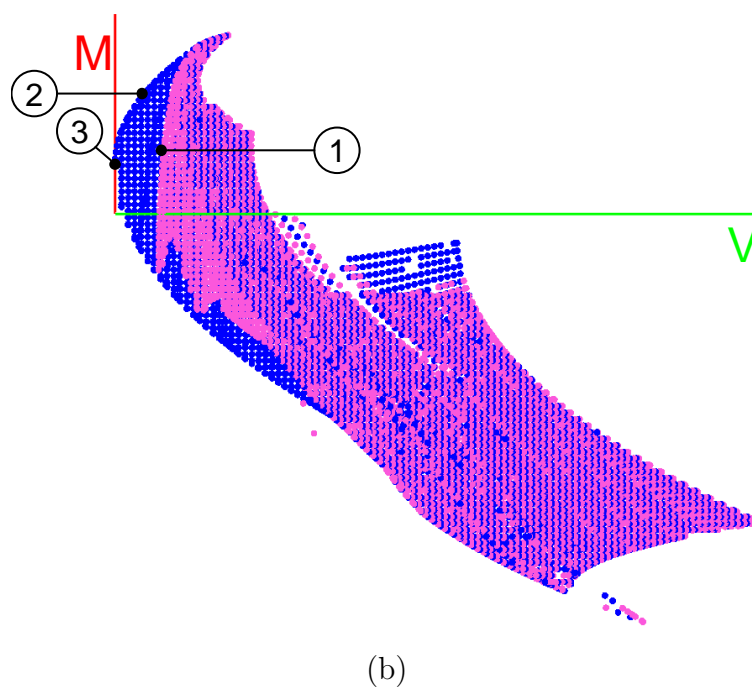
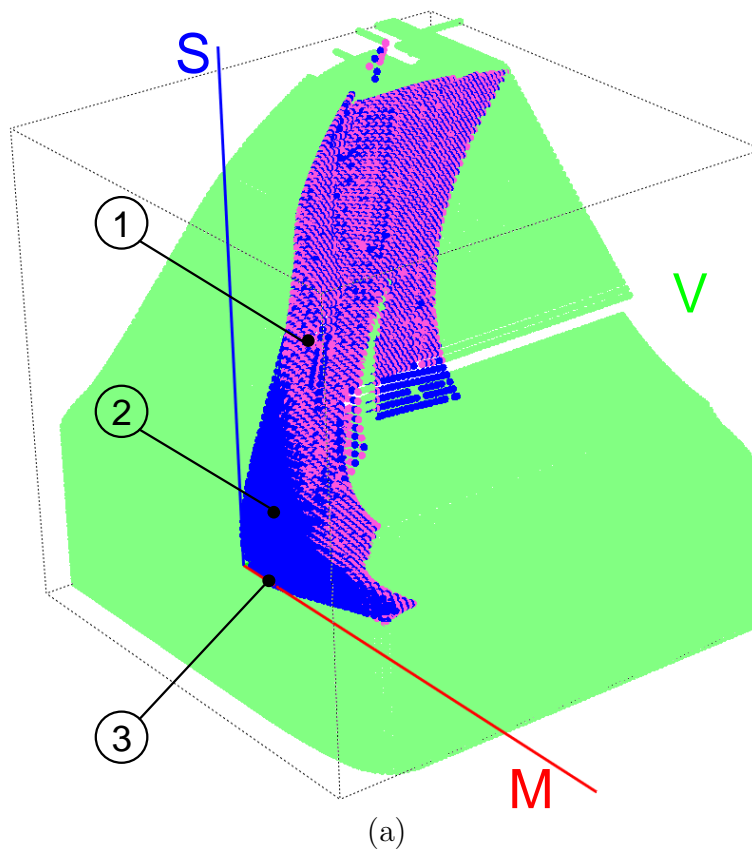


Figure 7: MV and MVS frontiers without and with risk-free rate

Table 1: MVS Model Contrasted with MV Model: Sample Level Results

Asset Nr.	Original data			MV Shortage			MVS Shortage			SkG	Shortage Function		MVS Färe-Lovell
	$E[R(x)]$	$\text{Var}[R(x)]$	$\text{Sk}[R(x)]$	$E[R(x)]$	$\text{Var}[R(x)]$	$\text{Sk}[R(x)]$	$E[R(x)]$	$\text{Var}[R(x)]$	$\text{Sk}[R(x)]$		MV	MVS	
1	0.0353	3.3627	2.3612	0.0344	1.5390	-0.7547	0.0353	3.3627	2.3612	1.2526	0.5423	0.0000	0.5423
2	-0.0544	6.7549	0.3514	-0.0094	1.1723	-0.2213	-0.0112	1.4044	-0.5297	1.3826	0.8265	0.7921	0.0344
3	0.0316	3.9695	-5.0237	0.0516	1.4656	-0.5951	0.0516	1.4656	0.6951	0.0000	0.6308	0.6308	0.0000
4	-0.0757	7.7454	-3.5315	-0.0105	1.1722	-0.2198	-0.0105	1.1722	-0.2198	0.0000	0.8487	0.8487	0.0000
5	-0.0907	4.2752	1.5169	-0.0105	1.1722	-0.2198	-0.0265	2.2919	2.2066	1.2537	0.7258	0.4639	0.2619
6	-0.1764	5.7799	-6.5307	-0.0105	1.1722	-0.2198	-0.0105	1.1722	-0.2198	0.0000	0.7972	0.7972	0.0000
7	-0.1005	6.5400	-14.8061	-0.0105	1.1722	-0.2198	-0.0105	1.1722	-0.2198	0.0000	0.8208	0.8208	0.0000
8	0.0236	4.7639	2.8948	0.0406	1.3383	-0.3960	0.0236	4.7639	2.8948	1.6072	0.7191	0.0000	0.7191
9	-0.0536	7.0233	-6.9667	-0.0089	1.1723	-0.2221	-0.0089	1.1723	-0.2221	0.0000	0.8331	0.8331	0.0000
10	-0.0100	2.7803	-0.4591	-0.0042	1.1739	-0.2305	-0.0042	1.1743	-0.1939	0.5409	0.5778	0.5776	0.0002
11	0.0094	4.5023	3.6677	0.0163	1.2096	-0.3156	0.0094	4.5023	3.6677	1.9058	0.7313	0.0000	0.7313
12	-0.0264	3.2672	0.2720	-0.0095	1.1723	-0.2213	-0.0104	1.3218	0.4340	1.3414	0.6412	0.5954	0.0458
13	-0.1076	6.9955	4.2525	-0.0105	1.1722	-0.2198	-0.0578	3.7547	6.2226	1.5991	0.8324	0.4633	0.3692
14	-0.0203	5.6006	-2.7488	-0.0042	1.1738	-0.2304	-0.0042	1.1738	-0.2304	0.0000	0.7904	0.7904	0.0000
15	-0.1508	12.8574	25.4645	-0.0105	1.1722	-0.2198	-0.1508	12.8574	25.4645	1.7319	0.9088	0.0000	0.9088
16	-0.0713	8.2059	10.1620	-0.0102	1.1722	-0.2202	-0.0606	6.9696	11.6931	1.5584	0.8571	0.1507	0.7065
17	-0.1202	9.4768	-19.4063	-0.0105	1.1722	-0.2198	-0.0105	1.1722	-0.2198	0.0000	0.8763	0.8763	0.0000
18	-0.1157	15.7459	22.9678	-0.0086	1.1724	-0.2227	-0.1157	15.4896	22.9710	1.2106	0.9255	0.0001	0.9254
19	-0.0588	6.2781	7.1303	-0.0105	1.1722	-0.2198	-0.0466	4.9764	8.6087	1.6234	0.8133	0.2073	0.6059
20	0.0488	3.0131	-7.5337	0.0647	2.0332	-1.5587	0.0647	2.0332	-1.5587	0.0000	0.3252	0.3252	0.0000
21	-0.1114	9.6308	13.3771	-0.0105	1.1722	-0.2198	-0.0937	8.0964	15.5084	1.7215	0.8783	0.1593	0.7190
22	-0.1015	3.6529	-4.2485	-0.0105	1.1722	-0.2198	-0.0105	1.1722	-0.2198	0.0000	0.6791	0.6791	0.0000
23	-0.1222	3.9361	-2.4225	-0.0105	1.1722	-0.2198	-0.0105	1.1722	-0.2198	0.0000	0.7022	0.7022	0.0000
24	0.0009	8.3625	5.3269	0.0017	1.1788	-0.2483	0.0009	8.3625	5.3269	2.3590	0.8590	0.0000	0.8590
25	-0.0612	4.7398	-3.0159	-0.0105	1.1722	-0.2198	-0.0105	1.1722	-0.2198	0.0000	0.7527	0.7527	0.0000
26	0.0718	2.7681	-0.9317	0.0718	2.7681	-0.9317	0.0718	2.7681	-0.9317	0.0000	0.0000	0.0000	0.0000
27	-0.1070	5.2393	-2.0284	-0.0105	1.1722	-0.2198	-0.0105	1.1722	-0.2198	0.0000	0.7763	0.7763	0.0000
28	0.0272	4.4182	3.2687	0.0459	1.3850	-0.4057	0.0272	4.4182	3.2687	1.6774	0.6865	0.0000	0.6865
29	-0.0938	8.1395	-6.8317	-0.0105	1.1722	-0.2198	-0.0105	1.1722	-0.2198	0.0000	0.8560	0.8560	0.0000
Average	-0.0545	6.2009	0.5699	0.0050	1.2944	-0.3397	-0.0138	3.5486	3.6401	0.7850	0.7315	0.4517	0.2798
St. Dev.	0.0653	3.0286	9.3743	0.0269	0.3354	0.2919	0.0483	3.6654	6.9645	0.8219	0.1900	0.3483	0.3565
Min	-0.1764	2.7681	-19.4063	-0.0105	1.1722	-1.5587	-0.1508	1.1722	-1.5587	0.0000	0.0000	0.0000	0.0000
Max	0.0718	15.7459	25.4645	0.0718	2.7681	-0.2198	0.0718	15.4896	25.4645	2.3590	0.9255	0.8763	0.9254

Note: The direction vector  $g$  is  $(|E[R(x)]|, -\text{Var}[R(x)], -\text{Sk}[R(x)])$  in the MV case and  $(|E[R(x)]|, -\text{Var}[R(x)], \text{Sk}[R(x)])$  in the MVS case.



Table 2: MV vs. MVS Model: Percent Changes for *American International Group*

	$\Delta$ Return (%)	$\Delta$ Variance (%)	$\Delta$ Skewness (%)
MV Efficiency	88.46	-72.58	-114.49
MVS Efficiency	70.77	-46.39	46.39

Table 3: Differences Between Projection Points of Shortage vs. Färe-Lovell Functions: Descriptive Statistics

	Return	Variance	Skewness
MAD	0.0485	1.9514	3.0771
Max	0.0718	15.3371	25.4645
Min	-0.1508	1.1722	-1.6547
Range	0.2226	14.1649	27.1192

# of valid points : 70639.

Table 4: Shortage Function: Slacks and Surplus Variables

	Slack in the direction of ...						Total with Slack	Total No Slack	Total
	M	V	S	MV	SM	SV			
#	7417	2346	21259	168	18736	4876	54802	16682	71484
%	10.38	3.28	29.74	0.24	26.21	6.82	76.66	23.34	100.00

Table 5: Angles of Projection: Shortage vs. Färe-Lovell Functions

	Angle in MV-plane		Angle in SM-plane		Angle in SV-plane	
	Shortage	Färe-Lovell	Shortage	Färe-Lovell	Shortage	Färe-Lovell
# angles	71484	71761	71484	71797	71484	71776
Average angle (°)	1.299	13.339	88.029	74.634	44.623	54.365
Standard deviation (°)	3.620	30.325	6.179	33.596	24.258	31.641
# 90° angles	0	9381	878	8978	0	11051
# 0° angles	877	7369	60	11430	60	10703
% 90° angles	0.00	13.07	1.23	12.50	0.00	15.40
% 0° angles	1.23	10.27	0.08	15.92	0.08	14.91

Table 6: Time Required to Generate Efficient Frontiers

Type of frontier	Type of grid	Nr of points	Time	Seconds per point
MVS with shortage function	2d-grid	30000	6m23s	0.013
MVS with shortage function	3d-grid	125000	20m14s	0.010
MVS with Färe-Lovell function	3d-grid	125000	24m13s	0.012
MV with shortage function	no grid	2900	10s	0.003